Energy 60 (2013) 453–456

Contents lists available at ScienceDirect

Energy

journal homepage: www.elsevier.com/locate/energy

Experimental studies of thermoelectric power generation in dynamic temperature environments

Peter M. Attia [a], Matthew R. Lewis [b], Cory C. Bomberger [b], Ajay K. Prasad [c], Joshua M.O. Zide [b, c, *]

[a] Department of Chemical and Biomolecular Engineering, University of Delaware, Newark, DE 19716, USA
[b] Department of Materials Science and Engineering, University of Delaware, Newark, DE 19716, USA
[c] Department of Mechanical Engineering, University of Delaware, Newark, DE 19716, USA

ARTICLE INFO

Article history:
Received 9 May 2013
Received in revised form
19 August 2013
Accepted 22 August 2013
Available online 17 September 2013

Keywords:
Thermoelectric
Thermoelectric power generation
Heat transfer
Heat exchangers
Heat engines

ABSTRACT

We show that thermoelectrics can generate power from environments experiencing temporal temperature fluctuations; this source of power is useful for low-power devices in remote locations. We design and characterize devices that employ a thermoelectric module sandwiched between two heat exchangers with significantly different thermal masses and examine the effects of heat exchanger size and material selection, period of oscillation of the environmental temperature fluctuations, and radiative heat transfer on the thermoelectric power output. We report maximum experimental power generation on the order of milliwatts using standard bismuth telluride thermoelectric modules in devices with a size of about 10 cm^3.

1. Introduction

Thermoelectric devices are capable of generating electric power given a temperature difference (ΔT) across the device. TPG (Thermoelectric power generation) is governed by the relation $P = (\alpha\Delta T)^2/R_{total}$, where α is the Seebeck coefficient and R_{total} is the sum of the internal and load resistances. A TPG device consists of a thermoelectric module between two heat exchangers. In the simplest case, the heat exchangers are thin ceramic plates that physically support the thermoelectric elements and aid in heat distribution. Some novel, high-performing thermoelectrics include doped semiconductors [1], semiconductors with buried epitaxial nanoparticles [2], and silicon nanowires [3]. Optimizing phonon scattering on the atomic scale, nanoscale, and mesoscale dramatically increases the efficiency of thermoelectric materials [4] and is the likely direction of future thermoelectric research.

The power output of thermoelectric devices is significantly affected by heat exchanger and thermoelectric module geometries. Previously studied heat exchanger geometries include fins exposed to air [5] and spirals, zig-zags, and fins directing a liquid heat transfer medium [6]. Most thermoelectric modules are either bulk-based or thin films [7]; a unique variant of bulk-based modules are two-stage, or stacked, modules [8]. Optimization studies of bulk thermoelectric elements [9] and thin films [10] detail the factors involved in maximizing the power output of thermoelectric devices.

Among other applications, thermoelectrics are often deployed in environments containing a steady-state spatial temperature gradient as a means of waste-heat recovery [11]. Because thermoelectric conversion efficiencies are on the order of 5% [12], thermoelectric waste-heat recovery applications are most competitive when considerations of reliability and high energy losses override cost and efficiency; such applications include industrial steam condensers [13] and remote oil pipelines [14]. Additionally, thermoelectric tailpipes and radiators in automobiles exploit waste heat from hot exhaust gas [15] and engine coolant [16], respectively, to power internal car electronics. Thermoelectrics have also been considered for applications in remote locations using natural temperature gradients such as those powered by direct [17] or concentrated [18] solar radiation [19] and those found in the ocean [20].

Using a heat transfer model, Bomberger et al. [21] showed that TPG in temporally-varying temperature environments can generate power by converting the temporal temperature fluctuations into a spatial temperature difference across the thermoelectric. This conversion is achieved by placing two heat exchangers with

* Corresponding author. 201 DuPont Hall, Newark, DE 19716, USA. Tel.: +1 302 831 3244.
E-mail address: zide@udel.edu (J.M.O. Zide).

0360-5442/$ – see front matter © 2013 Elsevier Ltd. All rights reserved.
http://dx.doi.org/10.1016/j.energy.2013.08.046

significantly different thermal inertias on either side of a thermoelectric plate. As the temperature of the environment changes with time, the temperature of each heat exchanger will respond at different rates, creating the spatial temperature difference required for power generation. TPG based on temporal temperature gradients is highly promising for small-scale power harvesting in remote environments where other power generation technologies are not practical. We report experimental results of TPG from dynamic temperature environments, verifying the aforementioned study's results [21], and determining the feasibility of TPG under different experimental conditions.

2. Experimental setup

2.1. Device characterization

We propose a simple relation to characterize these devices in an effort to optimize them for specific applications. By rearranging Newton's law of convection, $\dot{Q} = hA(T_a - T)$, and using a simple expression for the rate of temperature change of thermal mass, $\dot{Q} = \rho V C_p dT/dt$, a relationship is derived for the rate of temperature change of a heat exchanger primarily undergoing convective heat transfer:

$$\frac{dT}{dt} = \frac{h}{\rho C_p}\left(\frac{A}{V}\right)(T_a - T) = K(T_a - T) \quad (1)$$

where T, h, ρ, C_p, and A/V are the temperature, convective heat transfer coefficient, density, specific heat capacity, and surface area-to-volume ratio of the heat exchanger, respectively, T_a is the ambient temperature, and K is a proportionality constant termed the thermal response rate coefficient; all properties are assumed to be independent of temperature. Equation (1) is quantitatively accurate only for small heat exchangers with negligible internal temperature gradients, but its qualitative implications hold regardless of size. The thermoelectric power output depends strongly on the relative rates of temperature change of the two heat exchangers on either side of the thermoelectric plate, or K_{rapid}/K_{slow}. Clearly, the heat exchangers can be optimized with respect to geometry and material selection within the economic and size constraints of the application.

2.2. Device construction

Using this theory, we built five devices with varying heat exchanger sizes and configurations, as shown in Fig. 1. Consistent with Bomberger [21], a series of 10 cm long copper rods attached to a heat-spreading copper plate and a truncated quartz sphere were selected as the rapid and slow heat exchangers, respectively. The thermoelectric elements were composed of bismuth telluride, the industry standard thermoelectric material for low-temperature (<400 K) TPG applications [22]. The heat exchangers were bonded to the thermoelectric plate using thermally conductive silver epoxy. Acrylic support plates were constructed to secure the vertically upright copper rods; the supports were assumed to have a negligible effect on effective rod surface area and heat transfer coefficient. The devices were supported by various stands that minimally contact the quartz spheres, as shown in Fig. 1. Device specifications are given in Table 1; for ease of reference, each device is referred to by the diameter of its quartz sphere.

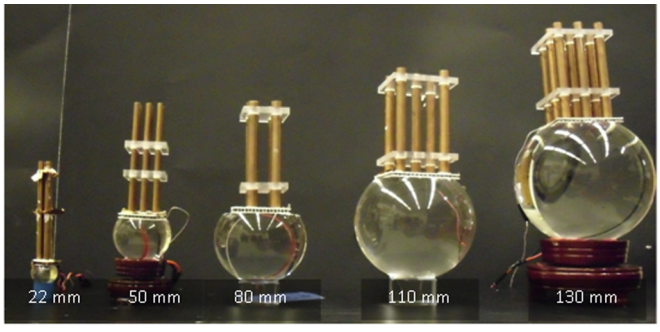

Fig. 1. Device geometries tested (labels indicate sphere diameters).

2.3. Experimental methodology

Each device was placed in a temperature-controllable chamber (Espec ECT) and connected to an external resistor approximately load-matched to the internal resistance of the thermoelectrics. After allowing the device to equilibrate at 34 °C, the temperature of the chamber was sinusoidally varied from 20 °C to 48 °C to match the amplitude of a diurnal cycle. The voltage across the resistor and the environmental temperature were logged using a digital multimeter (Keithley 2100) and a thermocouple data acquisition device (Omega TC-08). Power was calculated for each measurement using $P = V^2/R$.

3. Results and discussion

3.1. Comparison of experiment and simulation

The methods detailed in Bomberger [21] were used to create theoretical power profiles. Simple device properties, including the heat exchanger masses, thermoelectric Seebeck coefficients, and resistances, were measured experimentally. The heat transfer coefficients of the heat exchangers were found experimentally using the procedure given by Russell et al. [23]. Additionally, we chose to study radiative environments separately in order to obtain results for applications without solar radiation and reduce sources of experimental error, even though solar radiation was a significant component of the modeling study [21]. With these modifications, the model is in reasonable agreement with experiment without requiring the use of a fitting parameter. Experimental and theoretical power profiles for one device size (110 mm) are compared in Fig. 2 for an environmental oscillation period of 1 h, illustrating the close match between theory and experiment. As expected, the power profile exhibits a frequency that is double the oscillation frequency of the environmental temperature; the rapid heat exchanger is warmer than the slow heat exchanger during positive excursions of the environmental temperature, resulting in the first power peak, and cooler than the slow heat exchanger during negative excursions, resulting in the second power peak. The device generally takes about three cycles to attain dynamic equilibrium with the environmental temperature profile; therefore, the amplitudes of the first three power peaks of the power profile differ from those of subsequent peaks. The shape of the power profile approximately repeats after the first three peaks.

Table 1
Specifications of the five devices.

Sphere diameter (mm)	Sphere truncation distance (mm)	Number of copper rods	Copper rod diameter (mm)	Thermoelectric area (mm^2)	Number of thermoelectric couples
22	4	4	4.76	15 × 15	31
50	11	9	4.76	36 × 36	49
80	13	4	9.53	50 × 50	127
110	15	5	9.53	62 × 62	127
130	13	9	9.53	62 × 62	127

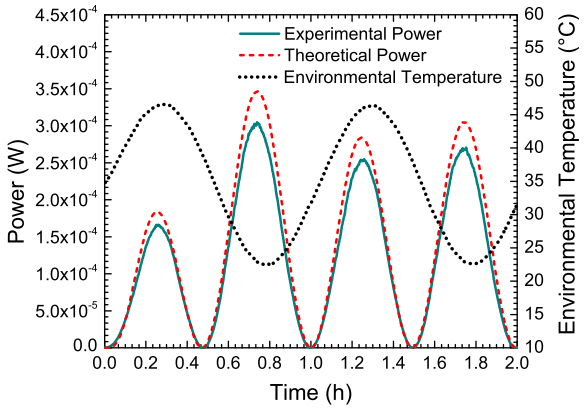

Fig. 2. Experimental and theoretical power profiles for the 110 mm device in a dynamic temperature environment and the corresponding environmental temperature profile. The period of the environment's sinusoidal temperature oscillation is 1 h.

3.2. Heat exchanger optimization

3.2.1. Size and geometry

The effect of heat exchanger size and geometry on power output was tested with the five device configurations (Table 1), of which the most significant geometric variation is the diameter of the quartz sphere. Since all five devices used the same heat exchanger materials and the value of h is roughly constant, the ratio of heat exchanger thermal response rate coefficients reduces to the ratio of heat exchanger surface area-to-volume ratios (A/V). Furthermore, since A/V of a sphere is inversely proportional to its radius, a larger quartz sphere corresponds to a smaller K_{slow}. Hence, the ratio K_{rapid}/K_{slow} increases for a given K_{rapid}, increasing the power generation. Increasing the device size (mostly by increasing the sphere radius but also the number and size of the copper rods and thermoelectric elements) generally increases the power output, as shown in Fig. 3. The power output eventually levels off with increasing device size for $K_{rapid}/K_{slow} > 3.5$.

3.2.2. Insulation

Another method of increasing the ratio of heat exchanger thermal response rate coefficients is to insulate the slow heat exchanger. Adding insulation reduces the thermal response rate coefficient of the quartz sphere, largely due to the reduction in its effective heat transfer coefficient. The spheres of the smallest and largest devices were wrapped in thin (3.175 mm) polyester insulation, although this method of attachment limited the number of layers of insulation that could be conformably added. The effect of insulation is illustrated by Fig. 4a where the theoretical average power is plotted against the quartz heat transfer coefficient for three values of the copper heat transfer coefficient. The average TPG decreases sharply for the particular value of the sphere's heat transfer coefficient at which K_{rapid}/K_{slow} approaches 1. At this point, the rates of temperature change for both heat exchangers are identical, so no power is generated. Fig. 4b shows the increase in measured TPG by adding layers of insulation to our smallest device (22 mm) for an oscillation period of 1 h. We observed an increase in average generated power per cycle from $5.9 \pm 0.8 \times 10^{-7}$ W to $1.9 \pm 0.1 \times 10^{-6}$ W with one layer of insulation on the quartz sphere and an increase to $7.45 \pm 0.04 \times 10^{-6}$ W with three layers of insulation for 1 h periods. With one layer of insulation on the quartz sphere of our largest device (130 mm), average TPG increased from 0.124 ± 0.004 mW to 0.160 ± 0.002 mW. Insulation is an effective means of improving device power output without dramatic increases in heat exchanger size.

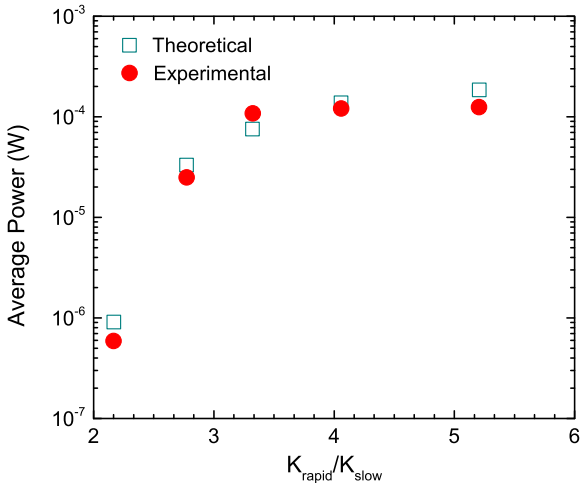

Fig. 3. Experimental and theoretical average TPG as a function of the ratio of thermal response rate coefficients of the two heat exchangers for an oscillation period of 1 h.

3.3. Environmental effects

3.3.1. Period of environmental temperature oscillation

To test the effect of the environmental temperature oscillation period on TPG, the power was measured for temperature chamber

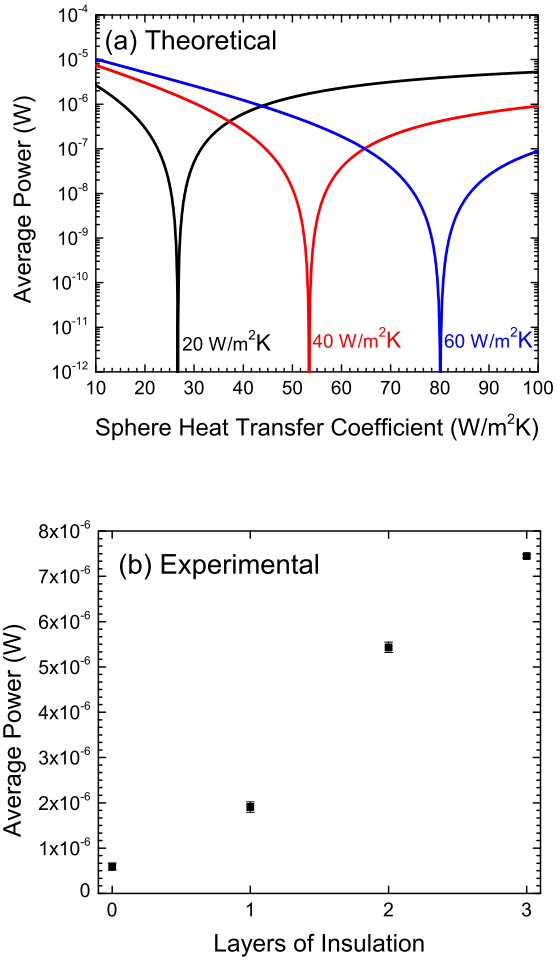

Fig. 4. (a) Simulated average power as a function of the quartz and copper heat transfer coefficients for the smallest device (22 mm) in an environment with a 1 h period of oscillation. Curves are presented for three values of copper heat transfer coefficient as denoted by the labels. (b) Experimental average power as a function of the number of layers of insulation on the 22 mm quartz sphere with a 1 h period of oscillation.

periods of 1, 3, and 5 h. The period of oscillation of the device's environment was found to be a significant factor in power output, as shown in Fig. 5. From theory, all of the devices produce maximum power if the period of oscillation is between 0.5 and 1 h. For oscillation periods smaller than the optimum, the environmental temperature is fluctuating too quickly for the temperature of the rapid heat exchanger to fully equilibrate, resulting in a small temperature difference across the thermoelectric plate. For oscillation periods larger than the optimum, both heat exchangers have sufficient time to come into thermal equilibrium with the environment, again resulting in a small temperature difference across the thermoelectric plate.

3.3.2. Simulated solar radiation

The effect of solar radiation on power output was also examined in conjunction with temperature oscillation. To simulate the spectrum of solar radiation, a halogen bulb rated for 70 W was placed inside the temperature chamber 24 cm away from the center of the copper heat exchanger. The quartz spheres of the devices were loosely wrapped in aluminum foil to limit radiative heat transfer to only one heat exchanger. Using pulse width modulation, the power to the bulb was sinusoidally varied from 0, to 70 W, and back to 0 for half of the period of temperature oscillation and set to 0 for the remaining half, approximating the solar cycle. The addition of radiative heat transfer to the copper rods increased TPG by 39%–98%, a range similar to that predicted by the model (45%–98%). The increase in power is due to the partially oxidized copper rods absorbing incident radiation during the positive temperature oscillations and the subsequent increase in the temperature difference across the thermoelectric.

4. Conclusion

In this study, we have experimentally verified TPG in a dynamic temperature environment and studied the effects of heat exchanger size, heat exchanger insulation, period of environmental temperature oscillation, and radiative heat transfer. Our largest average power outputs are on the order of 10^{-4} W, which is comparable to low-power thermoelectric applications for preamplifiers and sensor control systems [24] and radioisotope-powered probes for space exploration [25]. With optimization, thermoelectric devices (or any other heat engine) can be designed to provide power in other environments with temporal temperature fluctuations. The temperature fluctuations required to drive these devices can be either periodic, as studied here, or sporadic. This mechanism of generating power is applicable for any heat engine, not just thermoelectric devices. For an application requiring constant power, the generated power could be regulated by combining this device with an energy storage system. Some applications of this type of power source include sensors and signals in remote locations such as the desert and tracking large marine wildlife as they pass through oceanic thermoclines. Additionally, as thermoelectric efficiency continues to increase [4], the range of applications of these devices will expand.

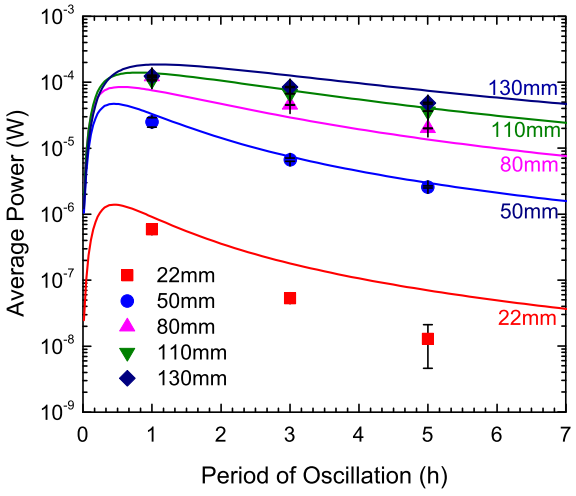

Fig. 5. Comparison of theoretical and experimental average TPG for different device geometries and periods of oscillation. Model predictions are represented by solid lines, and the corresponding experimental results are represented by symbols. Note that the experimental points for the largest two devices closely overlap.

Acknowledgments

Funding for this work is provided by the University of Delaware Strategic Initiatives Research Foundation and a Nanotechnology Undergraduate Education in Engineering grant (0939283) from the National Science Foundation.

References

[1] Dongmo P, Zhong Y, Attia P, Bomberger C, Cheaito R, Ihlefeld JF, et al. Enhanced room temperature electronic and thermoelectric properties of the dilute bismuthide InGaBiAs. J Appl Phys 2012;112:093710.
[2] Zide JM, Klenov DO, Stemmer S, Gossard AC, Zeng G, Bowers JE, et al. Thermoelectric power factor in semiconductors with buried epitaxial semimetallic nanoparticles. Appl Phys Lett 2005;87:112102.
[3] Hochbaum AI, Chen R, Delgado RD, Liang W, Garnett EC, Najarian M, et al. Enhanced thermoelectric performance of rough silicon nanowires. Nature 2008;451:163–7.
[4] Biswas K, He J, Blum ID, Wu C-I, Hogan TP, Seidman DN, et al. High-performance bulk thermoelectrics with all-scale hierarchical architectures. Nature 2012;489:414–8.
[5] Meng F, Chen L, Sun F. A numerical model and comparative investigation of a thermoelectric generator with multi-irreversibilities. Energy 2011;36:3513–22.
[6] Esarte J, Min G, Rowe DM. Modelling heat exchangers for thermoelectric generators. J Power Sources 2001;93:72–6.
[7] Benson DK, Tracy CE. Design and fabrication of thin film thermoelectric generators. In: Proceedings of the fourth international conference on thermoelectric energy conversion, Arlington, TX, USA 1982. p. 11–4.
[8] Chen L, Li J, Sun F, Wu C. Performance optimization of a two-stage semiconductor thermoelectric-generator. Appl Energy 2005;82:300–12.
[9] Chen L, Gong J, Sun F, Wu C. Effect of heat transfer on the performance of thermoelectric generators. Int J Therm Sci 2002;41:95–9.
[10] Mayer PM, Ram RJ. Optimization of heat sink-limited thermoelectric generators. Nanoscale Microscale Thermophys Eng 2006;10:143–55.
[11] Rowe D, Min G. Evaluation of thermoelectric modules for power generation. J Power Sources 1998;73:193–8.
[12] Riffat S, Ma X. Thermoelectrics: a review of present and potential applications. Appl Therm Eng 2003;23:913–35.
[13] Kyono T, Suzuki RO, Ono K. Conversion of unused heat energy to electricity by means of thermoelectric generation in condenser. IEEE Trans Energy Convers 2003;18:330–4.
[14] Bell LE. Cooling, heating, generating power, and recovering waste heat with thermoelectric systems. Science 2008;321:1457–61.
[15] Hsu C-T, Huang G-Y, Chu H-S, Yu B, Yao D-J. Experiments and simulations on low-temperature waste heat harvesting system by thermoelectric power generators. Appl Energy 2011;88:1291–7.
[16] Yang J, Stabler FR. Automotive applications of thermoelectric materials. J Electron Mater 2009;38:1245–51.
[17] Telkes M. Solar thermoelectric generators. J Appl Phys 1954;25:765.
[18] Kraemer D, Poudel B, Feng H-P, Caylor JC, Yu B, Yan X, et al. High-performance flat-panel solar thermoelectric generators with high thermal concentration. Nature Mater 2011;10:532–8.
[19] Chen J. Thermodynamic analysis of a solar-driven thermoelectric generator. J Appl Phys 1996;79:2717.
[20] Henderson J. Analysis of a heat exchanger – thermoelectric generator system. In: Intersociety energy conversion engineering conference, vol. 2. Boston, MA, USA: American Chemical Society; 1979. p. 1835–40.
[21] Bomberger CC, Attia PM, Prasad AK, Zide JMO. Modeling passive power generation in a temporally-varying temperature environment via thermoelectrics. Appl Therm Eng 2013;56:152–8.
[22] Rowe DM, Bhandarim CM. Modern thermoelectrics. Reston, VA, USA: Reston Publishing; 1983.
[23] Russell TWF, Robinson AS, Wagner NJ. Mass and heat transfer. 1st ed. New York, NY, USA: Cambridge University Press; 2008.
[24] Glosch H, Ashauer M, Pfeiffer U, Lang W. A thermoelectric converter for energy supply. Sens Actuators A Phys 1999;74:246–50.
[25] Bass J, Allen D. Milliwatt radioisotope power supply for space applications. In: Eighteenth international conference on thermoelectrics, Baltimore, MD, USA 1999. p. 521–4.